NARROWBAND AND WIDEBAND AMBIGUITY FUNCTIONS FOR SELECTED BARKER BINARY PHASE CODES

by

Jon Phillip Kjellander

United States Naval Postgraduate School

THESIS

NARROWBAND AND WIDEBAND AMBIGUITY FUNCTIONS

FOR SELECTED BARKER BINARY PHASE CODES

by

Jon Phillip Kjellander

October 1969

Narrowband and Wideband Ambiguity Functions for Selected Barker Binary Phase Codes

by

Jon Phillip Kjellander
Lieutenant (junior grade), United States Navy
B.S.E.E., Purdue University, 1968

Submitted in partial fulfillment of the
requirements for the degree of

MASTER OF SCIENCE IN ELECTRICAL ENGINEERING

from the

NAVAL POSTGRADUATE SCHOOL
October 1969

ABSTRACT

The Barker binary phase codes have the interesting property that the magnitude of the range sidelobes never exceeds 1/N, where N is the code length. This thesis presents ambiguity functions for certain selected Barker binary phase codes in the form of computer-drawn three-dimensional projections. Both the narrowband and wideband cases are taken into consideration.

TABLE OF CONTENTS

LIST OF TABLES

LIST OF ILLUSTRATIONS

ACKNOWLEDGEMENTS

I wish to thank Professor C. F. Klamm, Jr., for his assistance and his patience in the development of this thesis. It was Professor Klamm who interested me in the field of signal processing through his stimulating lectures.

I. INTRODUCTION

The key to any radar or sonar signal-processing system lies in the characteristics of the transmitted waveform, for no amount of signal processing can remove the fundamental limitations imposed by the waveform. It is the waveform that limits target resolution, causes ambiguities, and limits the accuracy in the estimation of parameters.

The basic signal parameters that may be varied are the energy, time duration, and bandwidth. Since there are many producers of noise, the ratio of the signal to the noise power spectral density must be sufficient to provide reliable detection. Once a signal of sufficient magnitude is detected, the process of parameter estimation may begin.

By far, the most common parameters estimated are range and velocity. The ambiguity function, originally defined by Woodward [1], gives a measure of the accuracy available for measuring range and velocity without ambiguities. It also expresses the ability of the system to resolve multiple targets.

In an attempt to get sufficient energy into the signal waveform for good detection characteristics, the time duration of the waveform is often increased. The results are twofold. The range resolution decreases while the velocity resolution increases. To increase the range resolution without changing the signal energy it is desirable to increase the signal bandwidth. One of the most common methods for increasing the signal bandwidth is the analog method of frequency modulation, or chirp radar.

The signal bandwidth may also be changed by digital methods, such as intrapulse modulation. The most common form of intrapulse modulation is phase modulation, which is illustrated in Figure 1-1. For example, a binary '0' may be represented by a 0° relative phase shift while a binary '1' may be represented by a relative phase shift of 180°. Figure 1-2 shows a typical matched filter for the binary phase codes.

With the idea of reducing range ambiguities and sidelobes, sonar and radar engineers have searched for binary codes that have good autocorrelation properties. One such set of codes is the complementary codes. The complementary codes have the interesting property that the autocorrelation functions for the codes have no range sidelobes. Pseudorandom codes also have good autocorrelation properties. Another set of codes with good autocorrelation functions is the set of Barker codes.

The normalized Barker codes have range sidelobes that never exceed 1/N in magnitude, where N is the code length, and have a magnitude of unity at the origin. The autocorrelation functions for all the known Barker codes are given in Figures 1-3a through 1-3c and 1-5a through 1-5f. Figure 1-4 is not a Barker code, but it was included explicitly to illustrate a code with large range sidelobes. The autocorrelation functions for the Barker codes are very easy to compute, since they are composed only of simple straight-line segments, and the verticies where they join are given by the equation: [2]

$$\chi(k) = \sum_{i=1}^{N-|k|} X_i X_{i+k} \quad ,$$

where

$$k = 0, \pm 1, \pm 2, \ldots, \pm(N-1)$$

and

N = code length.

It is the intent of this thesis to look at the ambiguity functions for some of the Barker binary phase codes for both the narrowband and wideband cases. The wideband case differs from the narrowband case by taking into consideration the effect of target motion in changing the shape of the echo return.

In Chapter II the narrowband ambiguity function is presented for the binary phase codes and the narrowband ambiguity functions for some of the Barker codes are plotted in the form of a computer-generated three-dimensional projection.

Chapter III presents a wideband analysis in which the effects of target motion on the waveshape are taken into consideration. Three-dimensional projections are given to show the changing of the ambiguity functions as the waveforms become wideband.

Chapter IV contains the summary of the results of the study, and also some recommendations for further investigation.

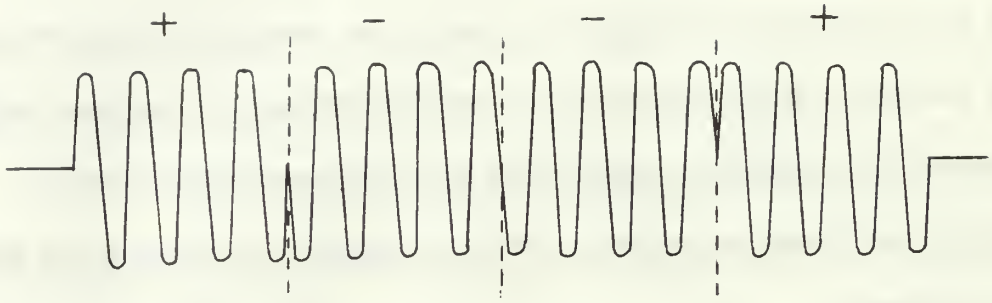

Fig. 1-1 BINARY PHASE-CODED WAVEFORM FOR THE CODE +--+

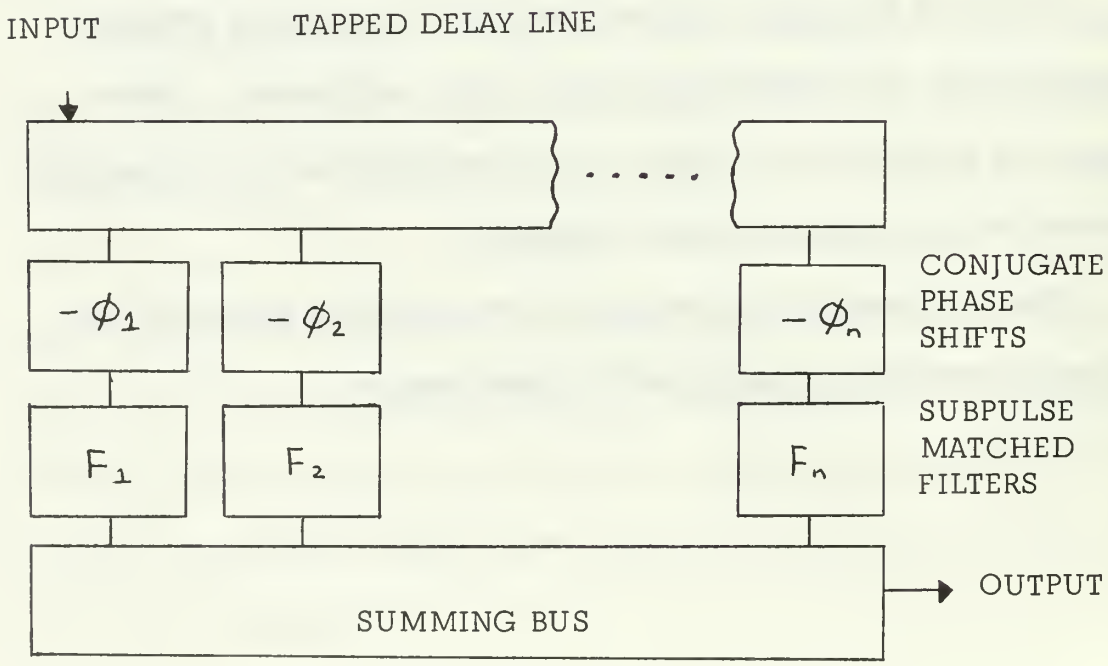

Fig. 1-2 MATCHED FILTER FOR THE BINARY PHASE-REVERSAL WAVEFORM

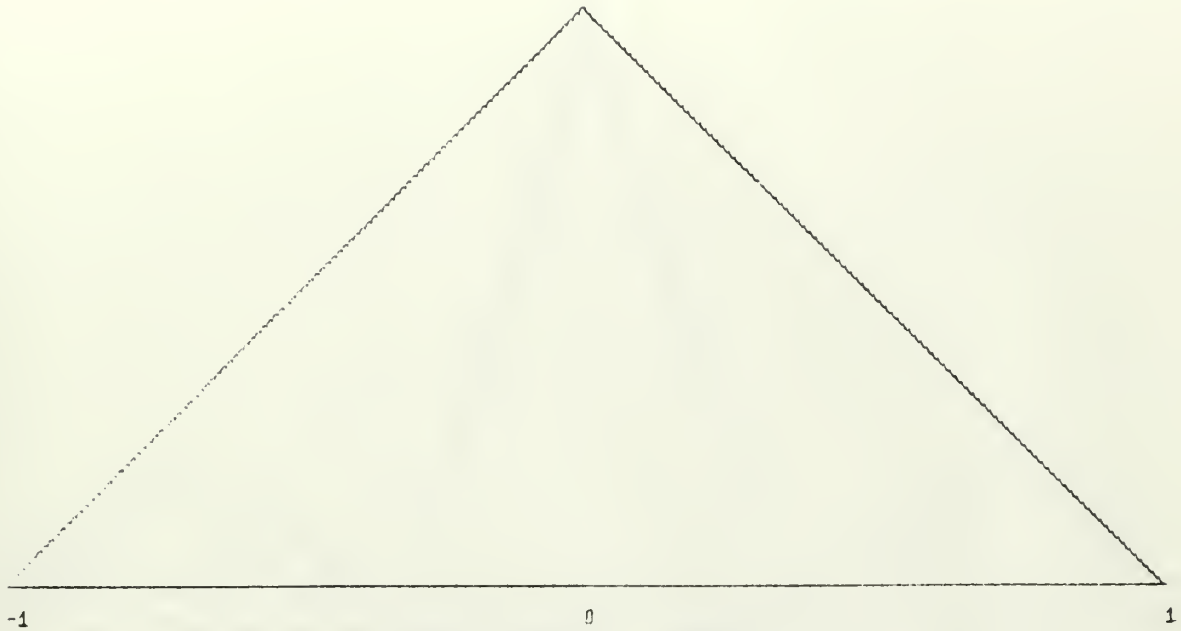

TIME SHIFT - TAU

FIGURE 1-3A AUTOCORRELATION FUNCTION MAGNITUDE FOR THE CODE 1

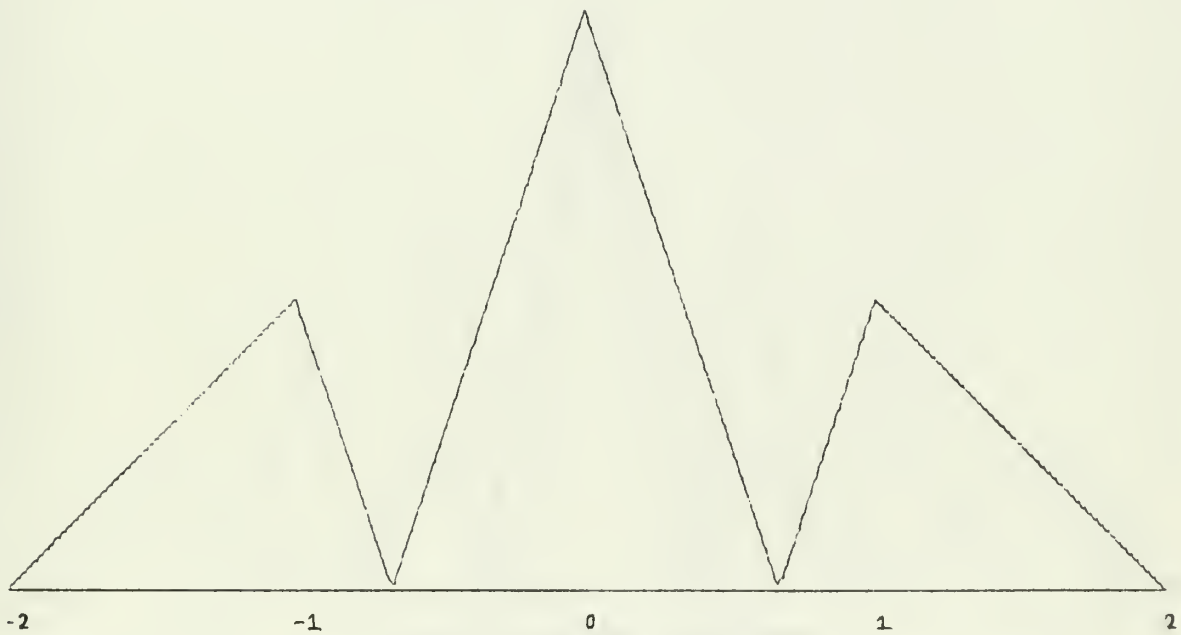

TIME SHIFT - TAU

FIGURE 1-3B AUTOCORRELATION FUNCTION MAGNITUDE FOR THE CODE 1 -1

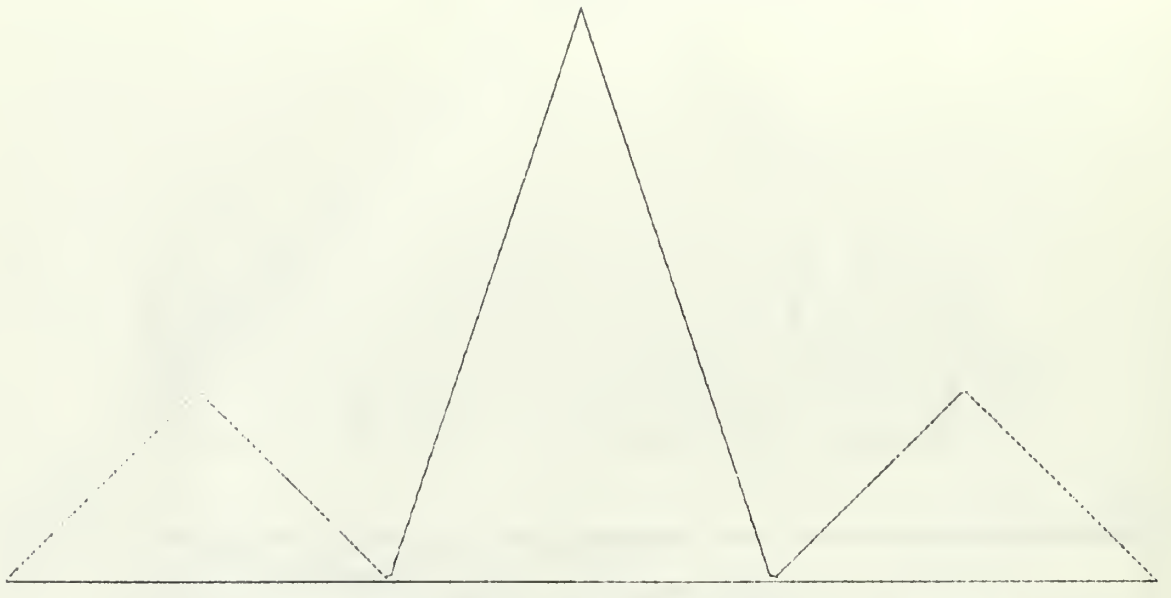

FIGURE 1-3C AUTOCORRELATION FUNCTION MAGNITUDE FOR THE CODE 1 1 -1

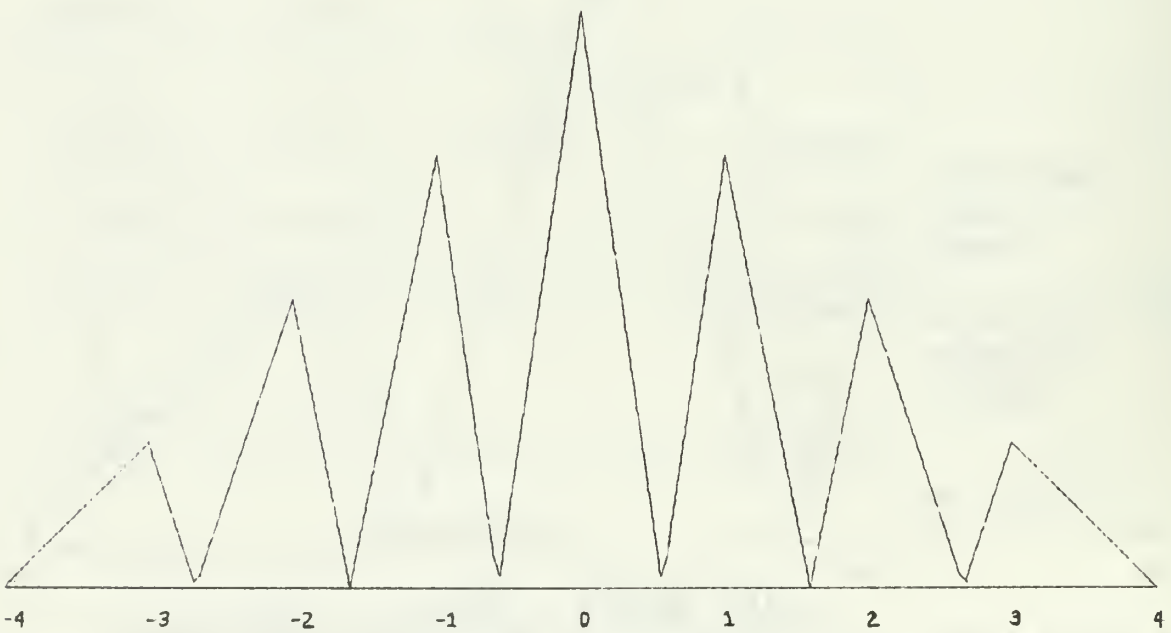

FIGURE 1-4 AUTOCORRELATION FUNCTION MAGNITUDE FOR THE CODE 1 -1 1 -1

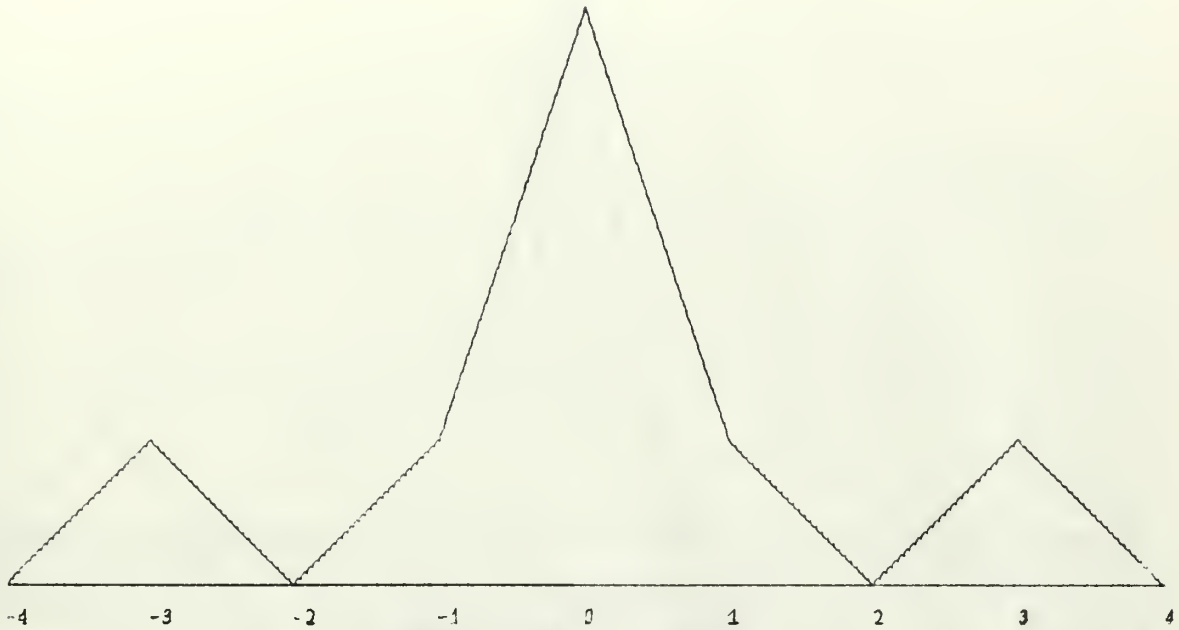

FIGURE 1-5A AUTOCORRELATION FUNCTION MAGNITUDE FOR THE CODE 1 1 1 -1

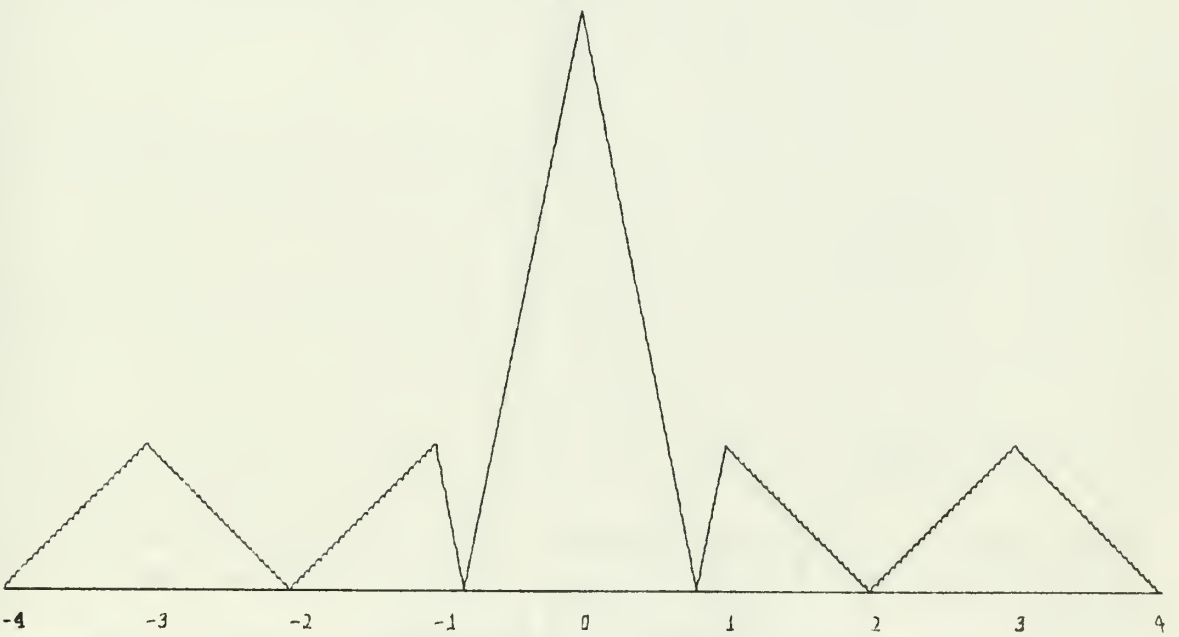

FIGURE 1-5B AUTOCORRELATION FUNCTION MAGNITUDE FOR THE CODE 1 1 -1 1

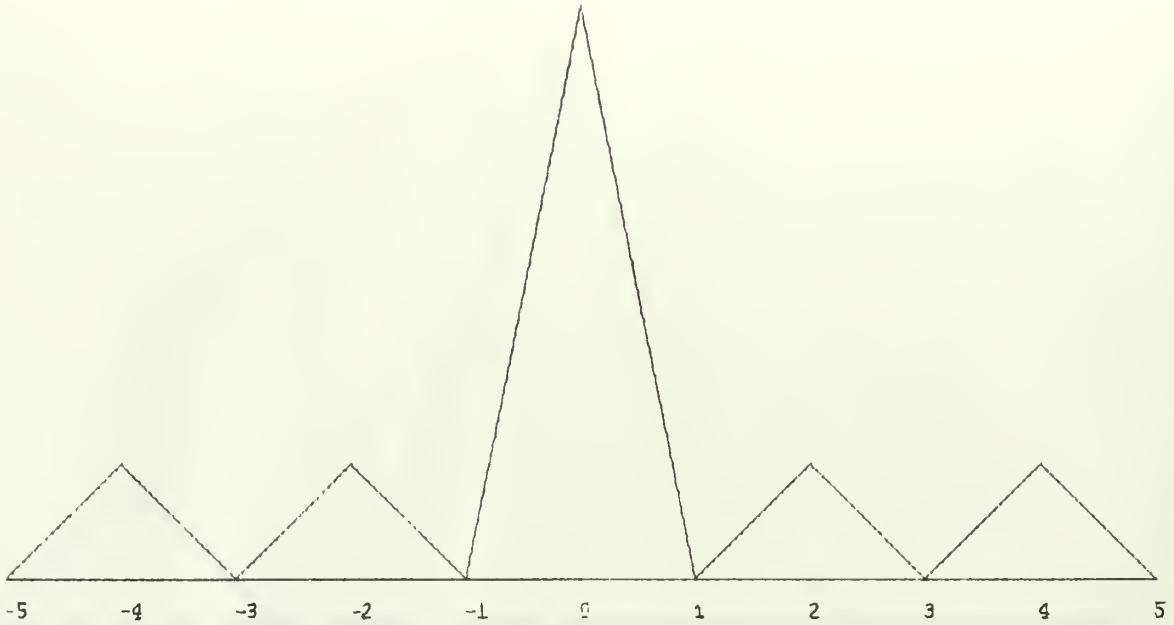

TIME SHIFT - TAU

FIGURE 1-5C AUTOCORRELATION FUNCTION MAGNITUDE FOR THE CODE 1 1 1 -1 1

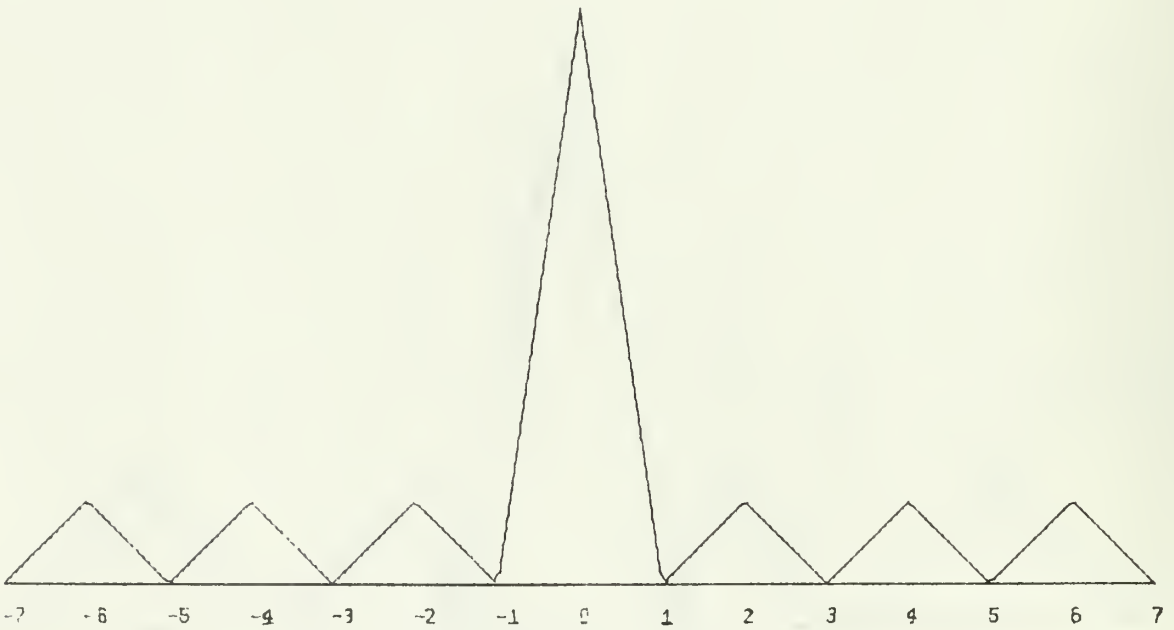

TIME SHIFT - TAU

FIGURE 1-5D AUTOCORRELATION FUNCTION MAGNITUDE FOR THE CODE 1 1 1 -1 -1 1 -1

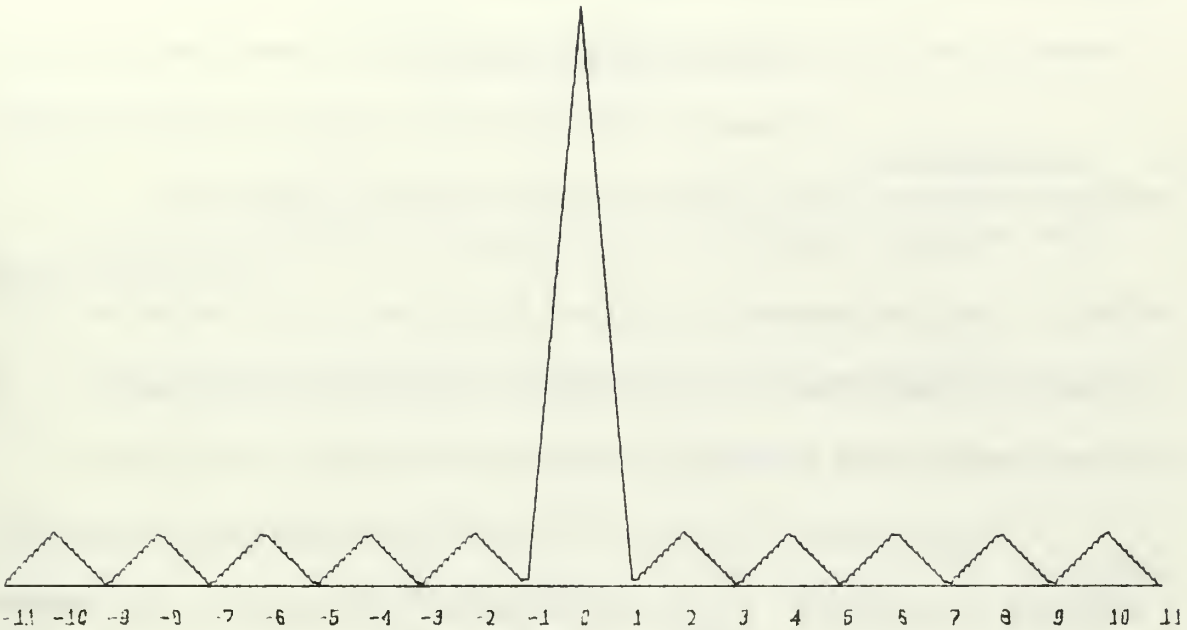

FIGURE 1-5E AUTOCORRELATION FUNCTION MAGNITUDE FOR THE CODE 1 1 1 -1 -1 -1 1 -1 -1 1 -1

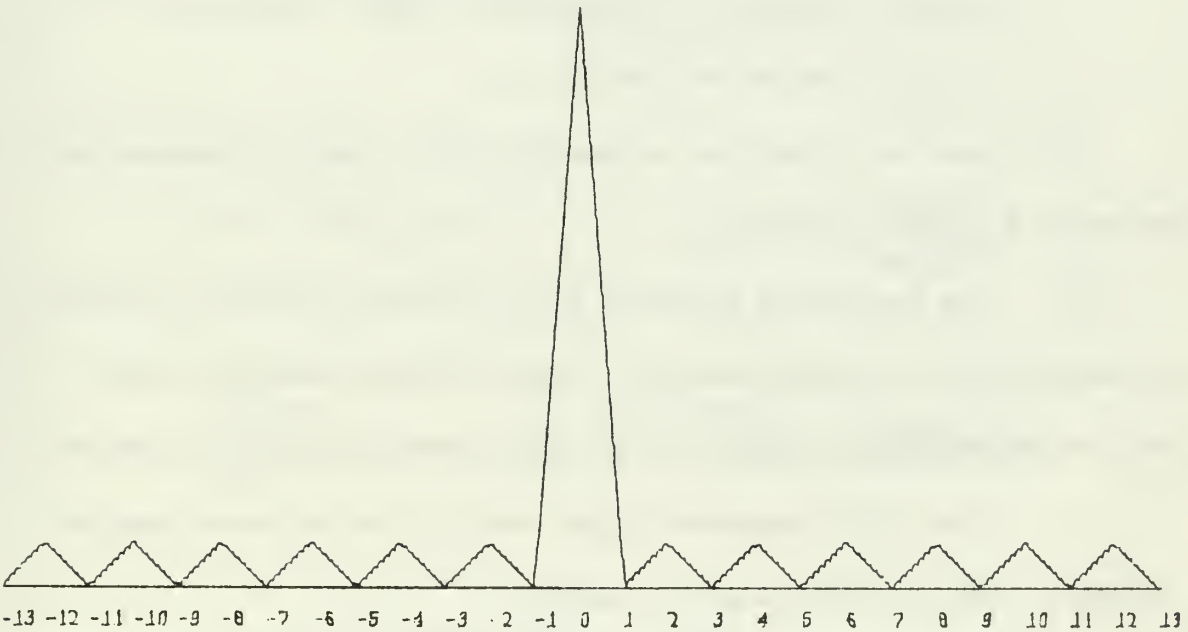

FIGURE 1-5F AUTOCORRELATION FUNCTION MAGNITUDE FOR THE CODE 1 1 1 1 1 -1 -1 1 1-11-11

II. NARROWBAND ANALYSIS

A. BACKGROUND

The ambiguity function was first defined by Woodward and was derived by applying Bayesian statistical techniques to the problem of optimum signal reception in the presence of white Guassian noise. Woodward defined his ambiguity function as:

$$\chi(\tau,\phi) = \int u(t)\, u^*(t+\tau) \exp(-j2\pi\phi t)\, dt \qquad 2\text{-}1$$

$$= \int U^*(f)\, U(f+\phi) \exp(-j2\pi f\tau)\, df$$

where

τ = time delay

ϕ = doppler shift

$u(t)$ = complex representation of signal modulation

$U(f)$ = Fourier transform of $u(t)$

It is important to realize the approximations used in deriving this ambiguity function:

1. The modulation waveform has a bandwidth which is narrow compared with the carrier frequency. Torres [3] indicates the upper limit for narrowband modulation to be about 5% of the carrier frequency.

2. The ratio of received signal energy to noise power spectral density is sufficient for reliable detection.

3. The receiver utilizes a crosscorrelation detection scheme.

4. The additive noise is white and Guassian.

5. Only the return of a single pulse is considered. This results in a continuous function as compared to the discrete line spectra found in pulse radars that have a pulse repetition frequency.

6. The effect of target motion is only to shift the center frequency of the echo return.

B. NARROWBAND AMBIGUITY FUNCTION FOR BINARY PHASE CODES

Akita [4] has derived the narrowband ambiguity function for the binary phase-reversal modulation waveforms from an extension of Siebert's [5] definition of the ambiguity function. Woodward's ambiguity function is identical to Siebert's ambiguity function with the exception that Siebert's function is real; in fact, it is the absolute value of Woodward's function. Akita's results were given by his equation 2-29:

$$\Psi(\tau,\omega_d) = \alpha^2 \left\langle \left\{ \frac{[(k+1)T-\tau]}{2} \frac{\sin \frac{\omega_d[(k+1)T-\tau]}{2}}{\frac{\omega_d[(k+1)T-\tau]}{2}} \sum_{i=1}^{N-k} X_i X_{i+k} \cdot \right.\right.$$

$$\cos \frac{\omega_d(2i+k-1)}{2} \div \frac{(\tau-kT)}{2} \frac{\sin \frac{\omega_d(\tau-kT)}{2}}{\frac{\omega_d(\tau-kT)}{2}} \cdot \qquad 2\text{-}2$$

$$\left. \sum_{i=1}^{N-(k+1)} X_i X_{i+k+1} \cos \frac{\omega_d(2i+k)T}{2} \right\}^2 + \left\{ \frac{[(k+1)T-\tau]}{2} \cdot \right.$$

$$\left. \frac{\sin \frac{\omega_d[(k+1)T-\tau]}{2}}{\frac{\omega_d[(k+1)T-\tau]}{2}} \sum_{i=1}^{N-k} X_i X_{i+k} \sin \frac{\omega_d(2i+k-1)T}{2} \right\rangle$$

$$+ \frac{(\tau - kT)}{2} \frac{\text{SIN} \frac{\omega_d(\tau - kT)}{2}}{\frac{\omega_d(\tau - kT)}{2}} \sum_{i=1}^{N-(k+1)} X_i \, X_{i+k+1} \cdot$$

$$\text{SIN} \frac{\omega_d(2i + k)T}{2} \Big]^2 \Big\rangle^{\frac{1}{2}} ,$$

where

N = length of the code

k = smallest integer $\geq \left| \frac{\tau}{T} \right|$

T = the duration of a code symbol

α = normalization constant $\sqrt{\frac{2}{NT}}$

$\tilde{\tau}$ = normalized time shift

ω_d = normalized doppler shift.

In order to avoid recomputing the ambiguity function for different waveform parameters, Akita suggested plotting the ambiguity function in terms of normalized time shift and doppler phase. The time shift is normalized by dividing by the duration of one code symbol, T. The doppler phase factor is defined as:

$$\Phi = \frac{W_d T}{2} = f_d T \pi \quad , \qquad 2\text{-}3$$

and is related to the radial velocity of the target by the narrowband approximation:

$$f_d \doteq \frac{2 V_r f_o}{C}, \qquad 2\text{-}4$$

which gives

$$V_r = \frac{C \, \Phi_d}{2 \pi f_o T}, \qquad 2\text{-}5$$

where

fo = carrier frequency

C = velocity of propagation

In order to realize the magnitudes of the parameters in the ambiguity function for both radar and sonar systems, Table 1 is presented on the following page.

Akita's equations were coded into FORTRAN IV and plotted using some of the three-dimensional techniques developed by Kennison [6]. The normalized doppler axis, omega, in the drawings is the same as Akita's doppler phase, Φ_d . By referring to the computer-generated drawings it will be easier to see the problems of resolution and ambiguity in a matched-filter signal-processing system.

The ambiguity function can be given physical interpretation and significance. The correlative signal processing which it embodies can be generated by either analog or digital means. Many of the practical radar systems in use today do not attempt to estimate target velocity from the doppler shift. In these systems the only effect of doppler shift is to reduce the output of the single matched filter employed, and the ambiguity function is equal to the envelope of the output of the matched filter.

TABLE 1

CONVERSION FROM DOPPLER PHASE, Φ_d, TO TARGETS RADIAL COMPONENT OF VELOCITY, Vr, FOR SONAR AND RADAR PARAMETERS

SONAR PARAMETERS

f_o = 1000Hz, T = 1 sec, C = 2.96×10^3 knots

Vr (knots)	(π rad)
.1	.0685
1.0	.685
10.0	6.85

RADAR PARAMETERS

f_o = 1 GHz, T = 1 sec, C = 5.91×10^8 knots

Vr (knots)	(π rad)
100	3.38×10^{-4}
5000	1.69×10^{-2}
60000	.2

For more sophisticated signal processing systems which are more often found in sonar systems in which estimates of both range and velocity are made, the ambiguity function has a little different meaning [7]. The return from a single point target will generate in a bank of matched filters, an output in each filter corresponding to the range and velocity of the target. If the number of matched filters is large, so that doppler response seems continuous, the envelope of the output of all the matched filters, as they are presented in terms of time shift, depicts the ambiguity function. In this context, each point target generates its own ambiguity function or interference in the signal processing system. To consider the resolution problems from multiple point targets, the ambiguity functions produced by the point targets may be added together, keeping in mind the requirement to scale each ambiguity function consistent with the strength of each point return. If the ambiguity functions intersect below the 3-db curve, the targets may arbitrarily be said to be resolved.

C. NARROWBAND AMBIGUITY FUNCTION DIAGRAMS

Figure 2-1a is the ambiguity function for the conventional pulsed CW waveform. The time axis forms the triangular autocorrelation function and is plotted in Figure 1-3a. The emergence of the autocorrelation function can be readily seen from Siebert's ambiguity function since:

$$\Psi(\tau,0) = \left| \int u(t)\, u(t+\tau)\, dt \right| \qquad 2\text{-}6$$

The doppler axis has a sin(x)/x characteristic which is the Fourier transform of the instantaneous power in a rectangular pulse envelope,

since:

$$\psi(0,\omega_d) = \int u(t)^2 \exp(j\omega_d t)\,dt \qquad 2\text{-}7$$

Notice the symmetry about the tau axis for the ambiguity function. Although it is not shown, the same reflective symmetry exists about the doppler axis.

Often it is desired to increase the range resolution of a waveform by decreasing the pulse duration. The first effect is to decrease the detection performance of the system since the criterion for optimum detection rests with the signal energy to noise power spectral density ratio. The second effect is to cause the sin(x)/x doppler axis to spread out, and thus decrease the doppler resolution.

One way to retain the detection characteristics, while at the same time improving the range resolution, is to utilize waveforms with a time-bandwidth product greater than unity. The pulsed CW waveform has a unity time-bandwidth product.

Figure 2-1b is the ambiguity function for the Barker code +-. This code has a time bandwidth product of two. Its autocorrelation function, shown in Figure 1-3b, shows a marked decrease in the width of the main range lobe; however, strong range sidelobes remain. The large range sidelobes are a problem since it may be difficult for a signal processing system to determine if a response is the result of a weak return or is a sidelobe of a strong return. It is interesting to note the symmetry that seems to be left over from the pulsed CW waveform. The ambiguity function for the code +- seems to be formed from the single-code ambiguity

function by splitting apart the single-code ambiguity function and introducing a series of mounds in the center along the time-shift axis. The ridges at the extremes of the tau axis are quite similar to those found in the single code ambiguity function.

Increasing the time bandwidth product to three with the code ++- generates the ambiguity function given by Figure 2-1c. Its autocorrelation function, given by Figure 1-3c, shows that the main range lobe is the same as in the previous code; however, the range sidelobes have decreased in magnitude. This ambiguity function bears much resemblence to the previous ambiguity function.

Increasing the time-bandwidth product to four with a non-Barker code illustrates the problem of ambiguities. This is shown by Figure 2-2. The autocorrelation function in Figure 1-4 shows how difficult it would be to determine the exact position of a target because of the broad response along the time-shift axis. A similar problem exists along the doppler axis. This waveform does little to help the resolution problem.

In contrast, Figure 2-3a is the ambiguity function for the Barker code +++-. Notice the similarities between this code and the code ++-. As the time-bandwidth product increases the Barker codes have the property that the range and velocity resolutions increase, while at the same time the ambiguities decrease.

Figure 2-3b is the ambiguity function for another Barker code of length four. It is interesting to note that the outlying ridges on either side of the extremes of the time-shift axis have the same form as found in previous ambiguity functions of the Barker codes.

The last ambiguity function plotted for a Barker code is shown in Figure 2-3c. This code has a time-bandwidth product of five and is almost identical to the ambiguity function for the code ++-+. The autocorrelation functions are also almost identical.

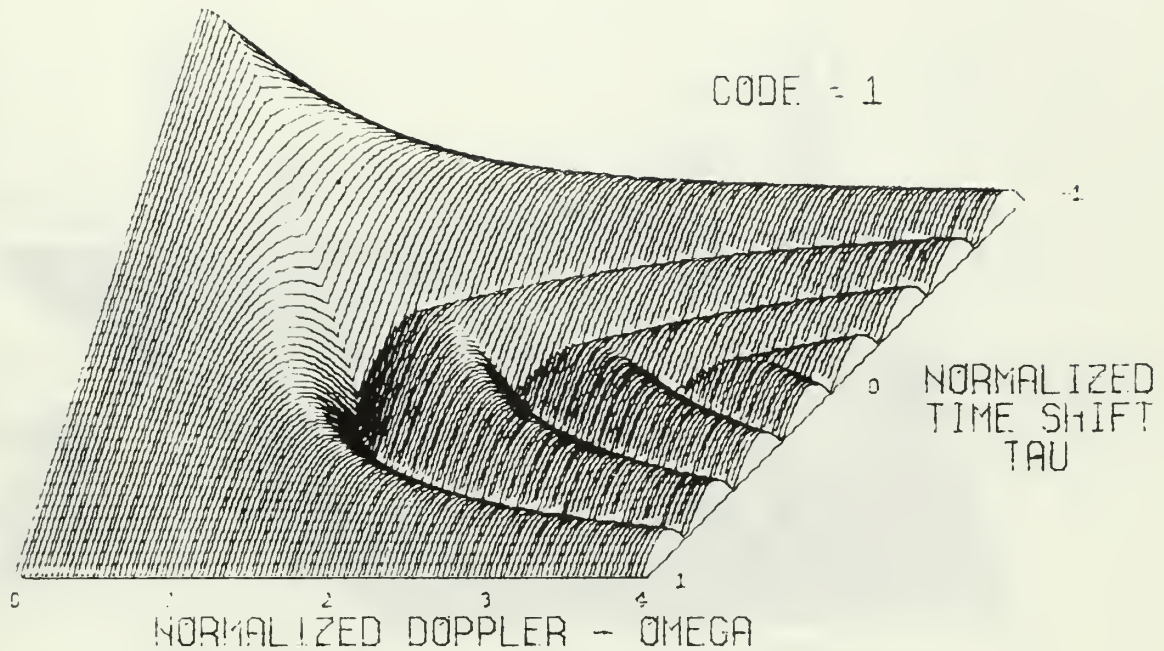

FIGURE 2-1A NARROWBAND AMBIGUITY FUNCTION

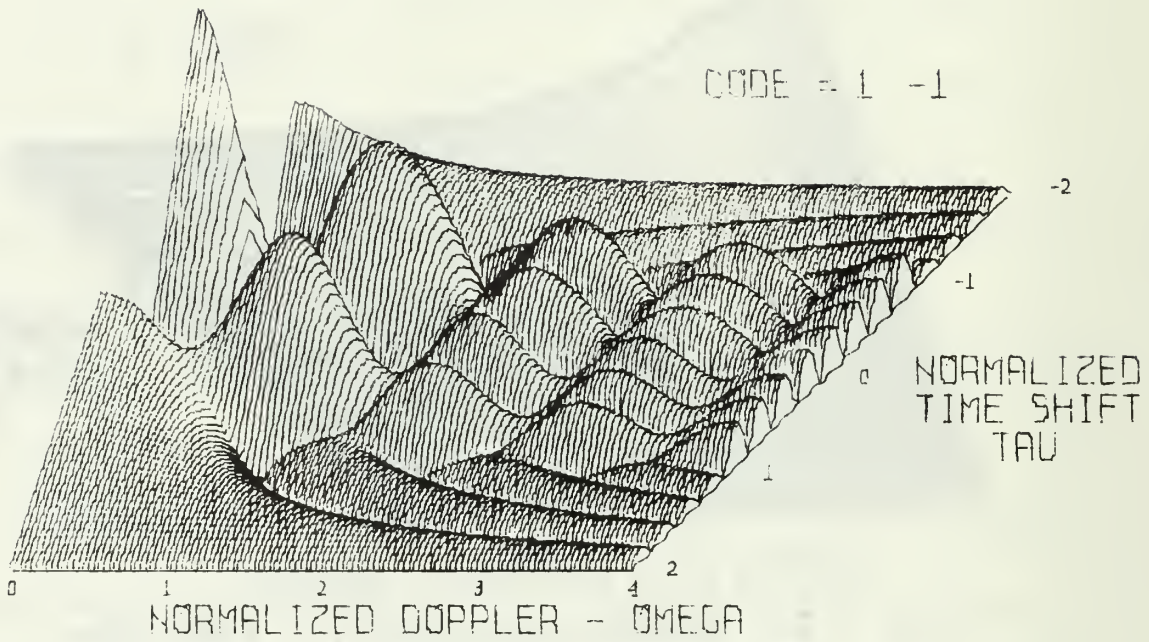

FIGURE 2-18 NARROWBAND AMBIGUITY FUNCTION

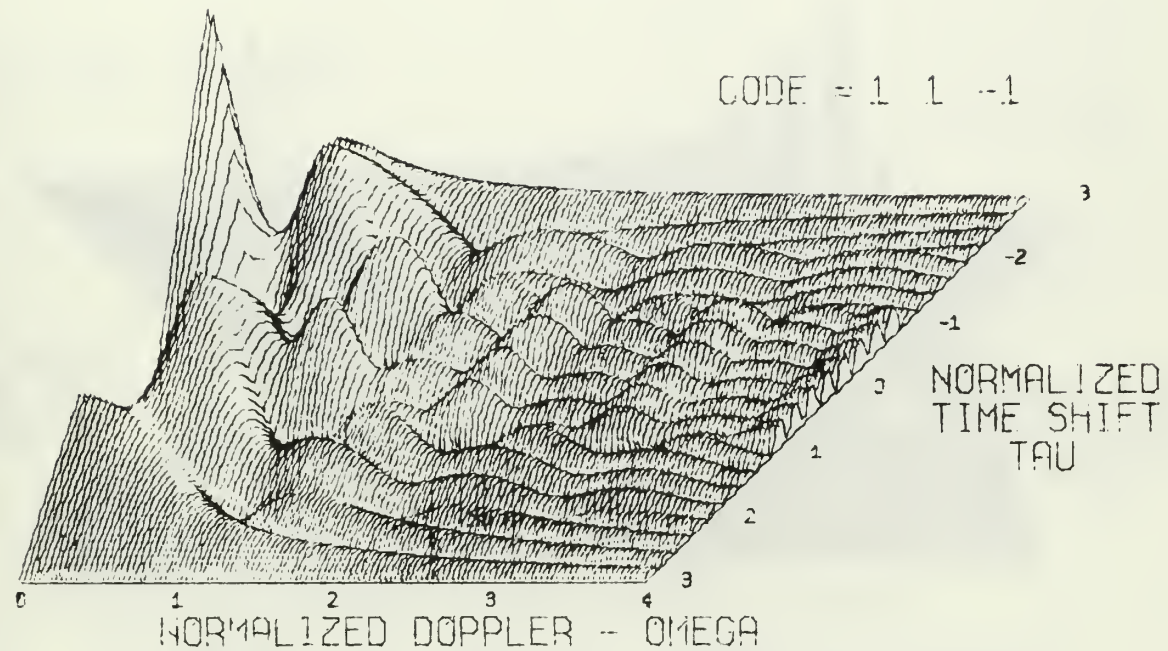

FIGURE 2-1C NARROWBAND AMBIGUITY FUNCTION

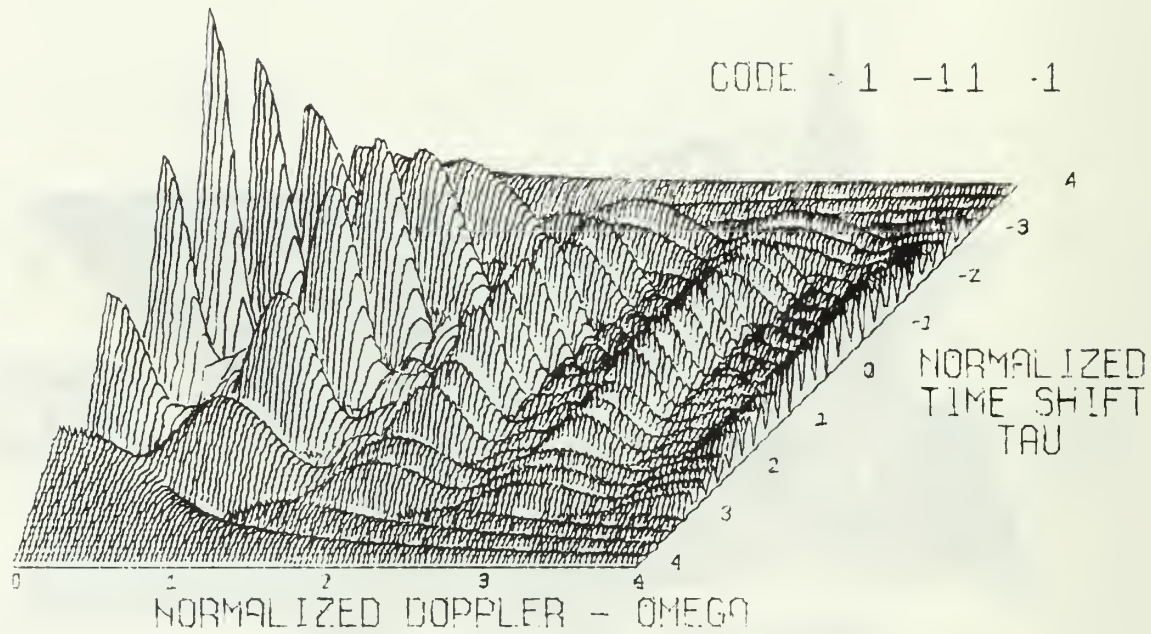

FIGURE 2-2 NARROWBAND AMBIGUITY FUNCTION

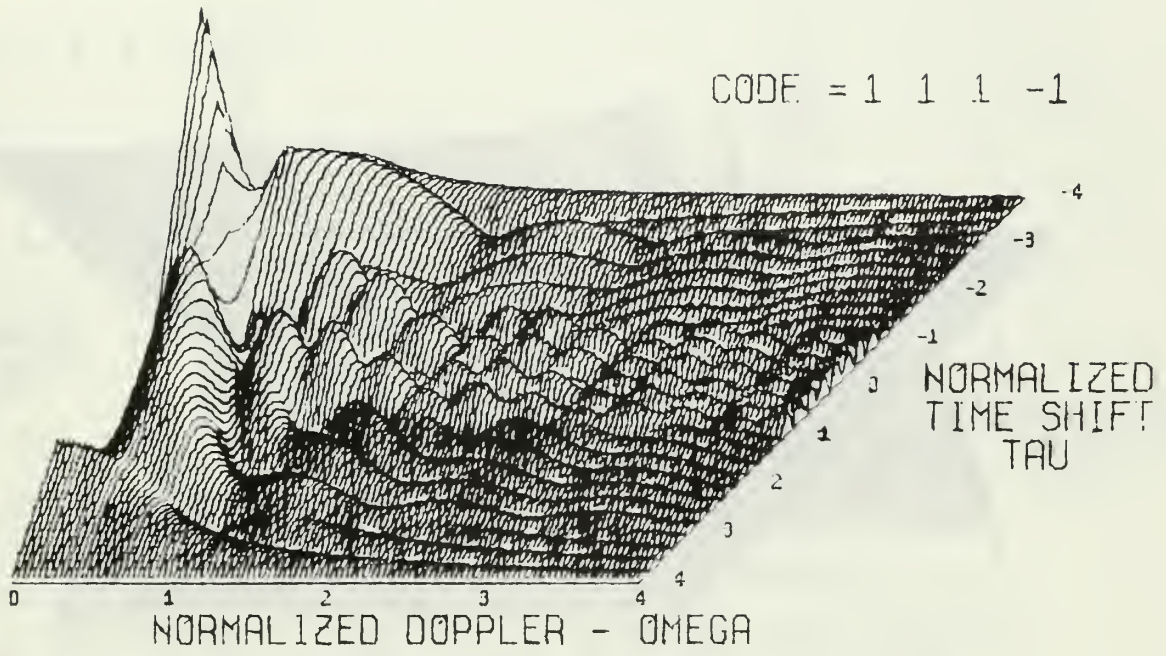

FIGURE 2-3A NARROWBAND AMBIGUITY FUNCTION

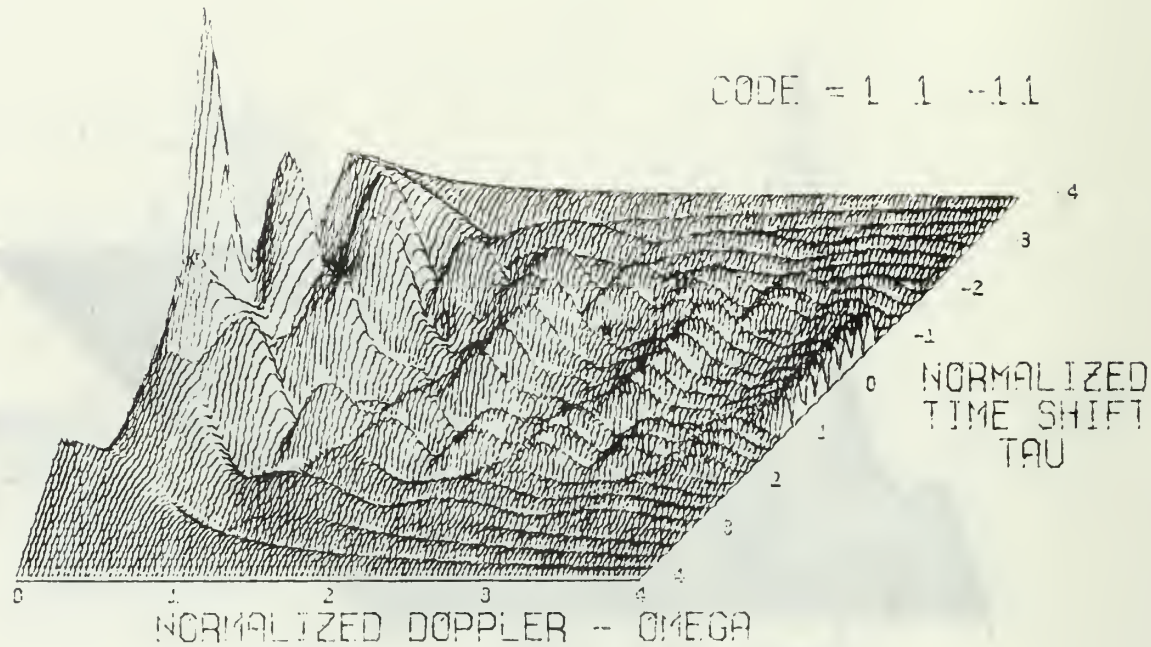

FIGURE 2-3B NARROWBAND AMBIGUITY FUNCTION

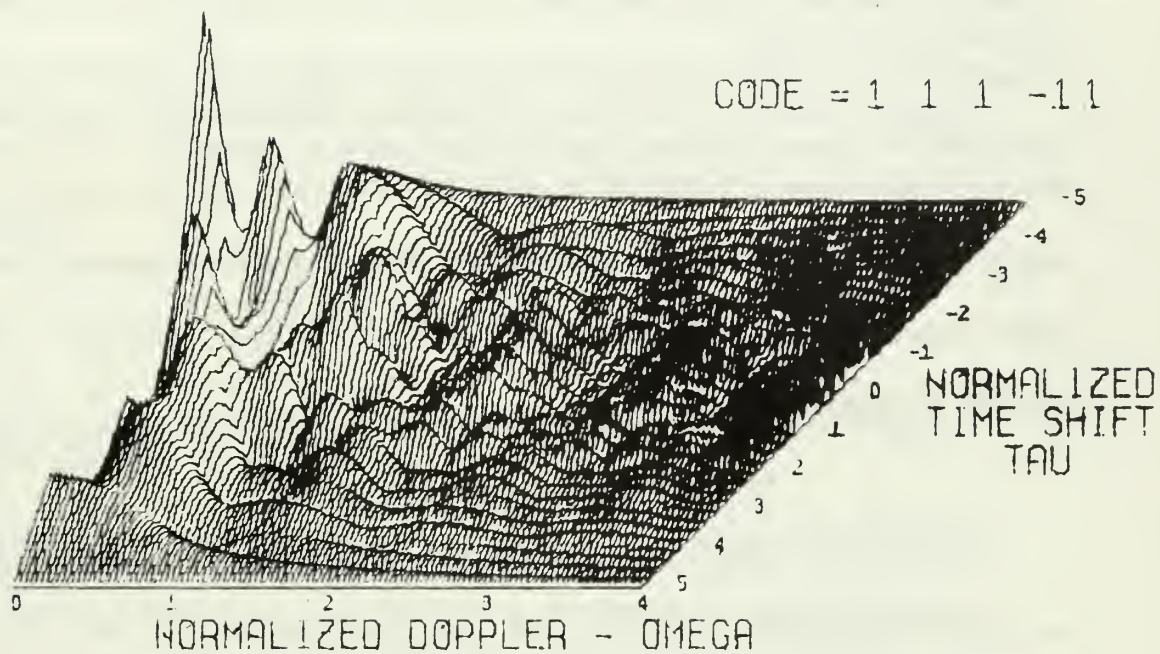

FIGURE 2-3C NARROWBAND AMBIGUITY FUNCTION

III. WIDEBAND ANALYSIS

A. BACKGROUND

In most practical cases in radar applications the effect of target motion is to simply shift the center frequency of the reflected signal. However, there exist important cases in which this approximation is no longer valid. In some sonar applications a relative velocity of only a few knots will be enough to invalidate the approximation of carrier frequency shift only.

One can see from the Fourier transform relationship, that if the signal frequencies are scaled by a factor, there will be an inverse factor introduced into the time domain. With a digital waveform this effect changes the time duration and amplitude of the pulse train. The transform relationship is:

$$\mathcal{F}^{-1}(S(f/D)) = Ds(Dt). \qquad 3\text{-}1$$

Kelly and Wishner [8] have established a criterion which separates the region for which the narrowband approximation is valid from the region in which the actual expansion or compression of the waveform must be taken into consideration.

When

$$\frac{2VrT\,B}{c} \ll 1, \qquad 3\text{-}2$$

the narrowband approximation is valid. Here

Vr = target radial velocity

c = velocity of wave propagation

T B = time-bandwidth product

As the time-bandwidth product is increased, for instance by using a longer Barker binary phase code, the region in which the narrowband approximation is valid is decreased. The time duration of the echo return will change by the doppler factor

$$D = \frac{1 + \frac{V_r}{c}}{1 - \frac{V_r}{c}} \doteq 1 + \frac{2V_r}{c} . \qquad 3\text{-}3$$

The change in time duration of the pulse train becomes important as the change approaches the duration of one code symbol. Since the time-bandwidth product of a Barker code is the same as the code length, N, equation 3-2 becomes

$$\frac{2V_r}{c} \ll \frac{1}{N} . \qquad 3\text{-}4$$

B. WIDEBAND AMBIGUITY FUNCTION FOR BINARY PHASE CODES FOR APPROACHING TARGETS

Akita has applied the time expansion and compression effect to the ambiguity function and has derived a wideband ambiguity function which is limited to a time expansion or contraction which is less than the duration of one code symbol. His equation 6-17 was defined as:

$$\Psi'(\tau,\omega) = \left| \frac{D_a}{2} \int I(D_a t_i) I(t_i - \tau) e^{j\omega_a t_i} dt_i \right| \qquad 3\text{-}5$$

Akita derived a wideband ambiguity function for the binary phase codes for the quadrant $W > 0, \tau > 0$. His equations 6-18, 19, 20, 21, and 22 are given below in their entirety:

1. For range deviations, τ, in the interval

$$(m-1)\frac{T'}{\Delta T} \leq \frac{\tau}{\Delta T} \leq \frac{T'}{\Delta T} - N + 1 - (m+1)\frac{T_{Di}}{\Delta T} \; ; \; m = 1, 2, \cdots N,$$

we have

$$\Psi'(\tau, \omega_\Delta) = \frac{D_\Delta \alpha^2}{2} \left| \sum_{i=1}^{N-p} X_i X_{i+p} \int_{\tau + (i-1)T_{Di}}^{(i+p)T'} e^{j\omega_\Delta t}\, dt \right.$$

$$\left. + \sum_{i=1}^{N-(p+1)} X_i X_{i+p+1} \int_{(i+p)T'}^{\tau + iT_{Di}} e^{j\omega_\Delta t}\, dt \right|, \qquad 3\text{-}6$$

where N = length of the code

$X_i = \pm 1$ depending on the ith value of the code symbol

D_i = replica signal's doppler factor = $1 + \frac{f_{di}}{f_o}$

D' = received signal's doppler factor = $1 + \frac{f_{d'}}{f_o}$

$$D_\Delta = \frac{D'}{D_i} = \frac{f_o + f_{d'}}{f_o + f_{di}}$$

$$\omega_\Delta = (D_\Delta - 1)\omega_o$$

T = transmitted signal's duration of a code symbol 3-7

T_{Di} = replica signal's duration of a code symbol = $\frac{T}{D_i}$

$T_{D'}$ = received signal's duration of a code symbol = $\frac{T}{D'}$

$$T' = \frac{T_{D'}}{D_\Delta}$$

ΔT = magnitude of the difference in the duration of a code symbol

$$= \left| T_{Di} - T' \right|$$

p = smallest integer $\geq \left| \frac{\tau}{T_{Di}} \right|$

j = -1 (denotes a complex quantity)

α = normalization constant = $\sqrt{\frac{2}{NT}}$.

Then if the integration is performed, equation 3-6 becomes

$$\Psi'(\tau,\omega_\Delta) = D_\Delta \alpha^2 \left| \sum_{i=1}^{N-p} X_i X_{i+p} \frac{[(i+p)T' - (i-1)T_{Di} - \tau]}{2} \cdot \right.$$

$$\frac{\text{SIN}\,\frac{\omega_\Delta[(i+p)T' - (i-1)T_{Di} - \tau]}{2}}{\frac{\omega_\Delta[(i+p)T' - (i-1)T_{Di} - \tau]}{2}} \; e^{j\frac{\omega_\Delta[(i+p)T' + (i-1)T_{Di}]}{2}}$$

$$+ \sum_{i=1}^{N-(p+1)} X_i X_{i+p+1} [\tau + iT_{Di} - (i+p)T'] \frac{\text{SIN}\,\frac{\omega_\Delta[\tau + iT_{Di} - (i+p)T']}{2}}{\frac{\omega_\Delta[\tau + iT_{Di} - (i+p)T']}{2}}$$

$$\left. e^{j\frac{\omega_\Delta[iT_{Di} + (i+p)T']}{2}} \right| . \qquad 3\text{-}8$$

2. For range deviations, τ , in the interval

$$\frac{T'}{\Delta T} - N + 1 + (m-1)\frac{T_{Di}}{\Delta T} \leq \frac{\tau}{\Delta T} \leq m\frac{T'}{\Delta T} \quad ; \quad m = 1, 2, \cdots, N \; ;$$

we have

$$\Psi'(\tau,\omega_\Delta) = \frac{D_\Delta \alpha^2}{2} \left| \sum_{i=1}^{n-h-k} X_i X_{i+k} \int_{\tau + (i-1)T_{Di}}^{(i+k)T'} e^{j\omega_\Delta t}\, dt \right.$$

$$+ \sum_{i=1}^{n-h-(k+1)} X_i X_{i+k+1} \int_{(i+k)T'}^{\tau + iT_{Di}} e^{j\omega_\Delta t}\, dt$$

$$\left. + X_{n-h-k} X_{n-h+1} \int_{(n-h)T'}^{(n-h+1)T'} e^{j\omega_\Delta t}\, dt \right.$$

$$+ \sum_{i=n-h}^{N-2} X_{i-k}\, X_{i+2} \int_{(i+1)T'}^{\tau+(i-k)T_{Di}} e^{j\omega_\Delta t}\, dt$$

$$+ \sum_{i=n-h}^{N-2} X_{i-k+1}\, X_{i+2} \int_{\tau+(i-k)T_{Di}}^{(i+2)T'} e^{j\omega_\Delta t}\, dt \Bigg|, \qquad 3\text{-}9$$

where the definitions in equation 3-7 apply and

$$n = \frac{T'}{\Delta T}$$

$$n_1 = \frac{T_{Di}}{\Delta T}$$

q = smallest integer $\geq \left|\frac{\tau}{\Delta T}\right|$

$h = q$ modulo (n_1)

k = smallest integer $\geq \left|\frac{\tau}{T_{Di}}\right|$

$f = q$ modulo (n).

If the integrals in equation 3-9 are evaluated, then the ambiguity function becomes

$$\Psi'(\tau, \omega_\Delta) = D_\Delta \alpha^2 \left| \sum_{i=1}^{n-h-k} X_i\, X_{i+k}\, \frac{[(i+k)T'-(i-1)T_{Di}-\tau]}{2} \right.$$

$$\left. \frac{\text{SIN}\, \frac{\omega_\Delta [(i+k)T'-(i-1)T_{Di}-\tau]}{2}}{\frac{\omega_\Delta [(i+k)T'-(i-1)T_{Di}-\tau]}{2}}\, e^{j\frac{\omega_\Delta [(i+k)T'+(i-1)T_{Di}]}{2}} \right|.$$

$$+ \sum_{i=1}^{n-h-(K+1)} X_i X_{i+K+1} \frac{[\tau + iT_{Di} - (i+K)T']}{2} \cdot$$

$$\frac{SIN \frac{\omega_\Delta [\tau + iT_{Di} - (i+K)T']}{2}}{\frac{\omega_\Delta [\tau + iT_{Di} - (i+K)T']}{2}} \quad e^{j \frac{\omega_\Delta [iT_{Di} + (i+K)T']}{2}}$$

$$+ X_{n-h-k} X_{n-h+1} \frac{T'}{2} \frac{SIN \frac{\omega_\Delta T'}{2}}{\frac{\omega_\Delta T'}{2}} e^{j \frac{\omega_\Delta [(2n-2h+1)T' - \tau]}{2}}$$

$$+ \sum_{i=n-h}^{N-2} X_{i-k} X_{i+2} \frac{[\tau + (i-k)T_{Di} - (i+1)T']}{2} \cdot$$

$$\frac{SIN \frac{\omega_\Delta [\tau + (i-k)T_{Di} - (i+1)T']}{2}}{\frac{\omega_\Delta [\tau + (i-k)T_{Di} - (i+1)T']}{2}} \quad e^{j \frac{\omega_\Delta [(i-k)T_{Di} + (i+1)T']}{2}}$$

$$+ \sum_{i=n-h}^{N-2} X_{i-k+1} X_{i+2} \frac{[(i+2)T' - (i+K)T_{Di} - \tau]}{2} \cdot \qquad 3-10$$

$$\frac{SIN \frac{\omega_\Delta [(i+2)T' - (i+K)T_{Di} - \tau]}{2}}{\frac{\omega_\Delta [(i+2)T' - (i+K)T_{Di} - \tau]}{2}} \quad e^{j \frac{\omega_\Delta [(i+2)T' + (i-K)T_{Di}]}{2}} \Bigg| .$$

Calculating the ambiguity function for the quadrant $\omega_\Delta > 0, \tau < 0$, in a manner similar to Akita's analysis, gives the following equations:

1. For range deviations, τ, in the interval

$$(m-1)T' + N\Delta T \leq \tau \leq mT_{oi} \quad ; \quad m = 1, 2, \cdots, N ;$$

we have

$$\Psi'(\tau, \omega_\Delta) = \frac{D_\Delta \alpha^2}{2} \left| \sum_{i=1}^{N-p} X_i X_{i+p} \int_{(i-1)T'}^{\tau + (i+p)T_{oi}} e^{j\omega_\Delta t} dt \right.$$

3-11

$$\left. + \sum_{i=1}^{N-(p+1)} X_i X_{i+p+1} \int_{\tau + (i+p)T_{oi}}^{iT'} e^{j\omega_\Delta t} dt \right| .$$

Integrating equation 3-11 gives:

$$\Psi'(\tau, \omega_\Delta) = D_\Delta \alpha^2 \left| \sum_{i=1}^{N-p} X_i X_{i+p} \frac{[\tau + (i+p)T_{oi} - (i-1)T']}{2} \cdot \right.$$

$$\frac{\text{SIN} \; \frac{\omega_\Delta [(\tau + (i+p)T_{oi} - (i-1)T']}{2}}{\frac{\omega_\Delta [(\tau + (i+p)T_{oi} - (i-1)T']}{2}} \cdot$$

$$e^{j \frac{\omega_\Delta [(i+p)T_{oi} + (i-1)T']}{2}}$$

$$\left. + \sum_{i=1}^{N-(p+1)} X_i X_{i+p+1} \frac{[iT' - \tau - (p+i)T_{oi}]}{2} \cdot \right|$$

$$\frac{\text{SIN}\ \frac{\omega_\Delta [iT' - \tau - (p+i)T_{Di}]}{2}}{\frac{\omega_\Delta [iT' - \tau - (p+i)T_{Di}]}{2}} \cdot$$

$$e^{j\frac{\omega_\Delta [iT' + (p+i)T_{Di}]}{2}} \Bigg| \qquad 3\text{-}12$$

2. For range deviations in the interval

$$(m-1)T_{Di} \leq \tau \leq (m-1)T' + N\Delta T \; ; \; m = 1, 2, \cdots, N$$

we have

$$\Psi'(\tau, \omega_\Delta) = \frac{D_\Delta \alpha^2}{2} \Bigg| \sum_{i=(q+2)\,\text{modulo}(n_1)}^{N-p} X_i X_{i+p} \int_{\tau+(i+p-1)T_{Di}}^{iT'} e^{j\omega_\Delta t}\, dt$$

$$+ \sum_{i=(q+2)\,\text{modulo}(n_1)}^{N-p} X_i X_{i+p-1} \int_{(i-1)T'}^{\tau+(i+p-1)T_{Di}} e^{j\omega_\Delta t}\, dt$$

$$+ \sum_{i=1}^{k} X_i X_{i+p+1} \int_{\tau+(i+p)T_{Di}}^{iT'} e^{j\omega_\Delta t}\, dt$$

$$+ \sum_{i=1}^{k} X_i X_{i+p} \int_{(i-1)T'}^{\tau+(i+p)T_{Di}} e^{j\omega_\Delta t}\, dt \qquad 3\text{-}13$$

$$+ X_{h+1} X_{f+1} \int_{hT'}^{(h+1)T'} e^{j\omega_\Delta t}\, dt$$

Integrating equation 3-13 gives:

$$\Psi(\tau,\omega_\Delta) = D_\Delta \alpha^2 \left| \sum_{i=(q+2)\,\mathrm{modulo}(n_1)}^{N-P} X_i X_{i+p} \frac{[iT'-(i+p-1)T_{Di}-\tau]}{2} \right.$$

$$\frac{\mathrm{SIN}\,\frac{\omega_\Delta[iT'-(i+p-1)T_{Di}-\tau]}{2}}{\frac{\omega_\Delta[iT'-(i+p-1)T_{Di}-\tau]}{2}} \; e^{j\frac{\omega_\Delta[iT'+(i+p-1)T_{Di}]}{2}}$$

$$+ \sum_{i=(q+2)\,\mathrm{modulo}(n_1)}^{N-P} X_i X_{i+p-1} \frac{[\tau+(i+p-1)T_{Di}-(i-1)T']}{2} \cdot$$

$$\frac{\mathrm{SIN}\,\frac{\omega_\Delta[\tau+(i+p-1)T_{Di}-(i-1)T']}{2}}{\frac{\omega_\Delta[\tau+(i+p-1)T_{Di}-(i-1)T']}{2}} e^{j\frac{\omega_\Delta[(i+p-1)T_{Di}+(i-1)T']}{2}}$$

$$+ \sum_{i=1}^{k} X_i X_{i+p+1} \frac{[iT'-(i+p)T_{Di}-\tau]}{2} \cdot$$

$$\frac{\mathrm{SIN}\,\frac{\omega_\Delta[iT'-(i+p)T_{Di}-\tau]}{2}}{\frac{\omega_\Delta[iT'-(i+p)T_{Di}-\tau]}{2}} e^{j\frac{\omega_\Delta[iT'+(i+p)T_{Di}]}{2}}$$

$$+ \sum_{i=1}^{k} X_i X_{i+p} \frac{[\tau+(i+p)T_{Di}-(i-1)T']}{2} \cdot$$

$$\frac{\sin \frac{\omega_\Delta [\tau + (i+p)T_{Di} - (i-1)T']}{2}}{\frac{\omega_\Delta [\tau + (i+p)T_{Di} - (i-1)T']}{2}} \; e^{j\frac{\omega_\Delta [(i+p)T_{Di} + (i-1)T']}{2}}$$

3-14

$$+ \; X_{h+1} \, X_{f+1} \, \frac{T'}{2} \, \frac{\sin \frac{\omega_\Delta T'}{2}}{\frac{\omega_\Delta T'}{2}} \; e^{j\omega_\Delta \frac{[(2h+1)T' - \tau]}{2}} .$$

C. WIDEBAND AMBIGUITY FUNCTION FOR SELECTED BARKER CODES

Equations 3-8, 3-10, 12, and 14 were programmed in FORTRAN IV and plotted using various carrier-frequency X clock-period products. The carrier-frequency X clock-period product is indicated on the computer drawn plots as FO*T. or fo times T.

Figure 3-1a has a FO*T of 1000. This is the same function as the narrowband function presented earlier. Changing the FO*T product tenfold as in Figure 3-1b has only the effect of stretching the function a slight amount on the omega-delta axis. Figure 3-1c shows the function to be stretching and also starting to shift away from the tau = 1 line. Figures 3-1d,e, and f show the same effects to be more pronounced. Figure 3-1g is for the Barker code +-. In all the wideband ambiguity function plots there seems to exist a symmetry about a line which is through the origin and skewed by translation along the tau axis by an amount equal to the difference in the length between the compressed and uncompressed pulse trains. In addition, compression in the tau direction has also been introduced.

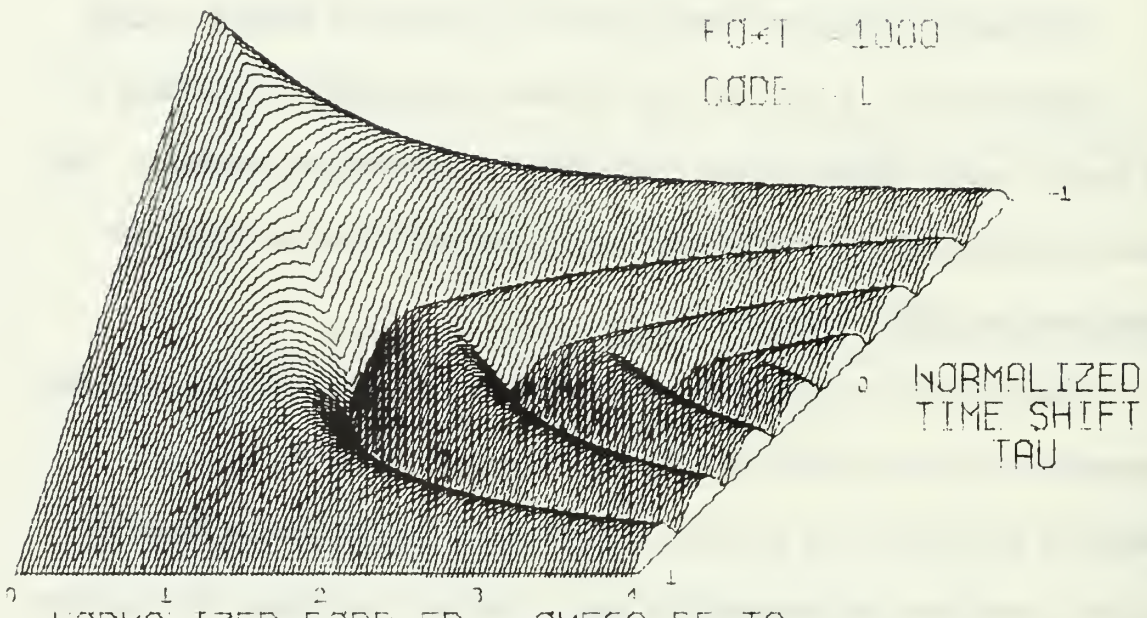

FIGURE 3-1A WIDEBAND AMBIGUITY FUNCTION

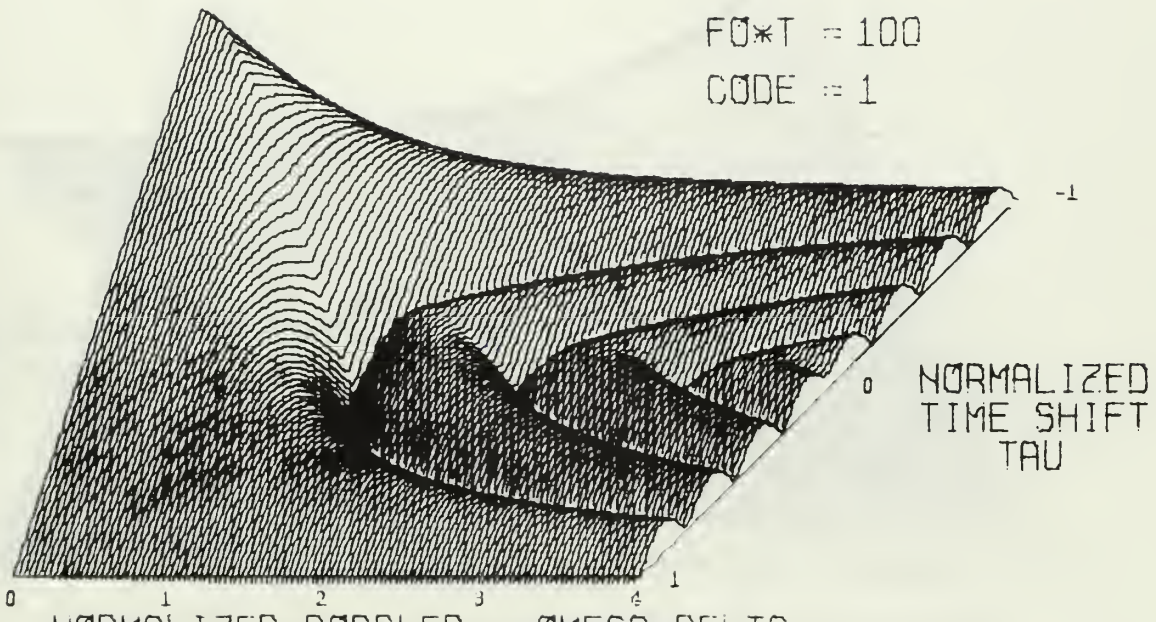

FIGURE 3-1B WIDEBAND AMBIGUITY FUNCTION

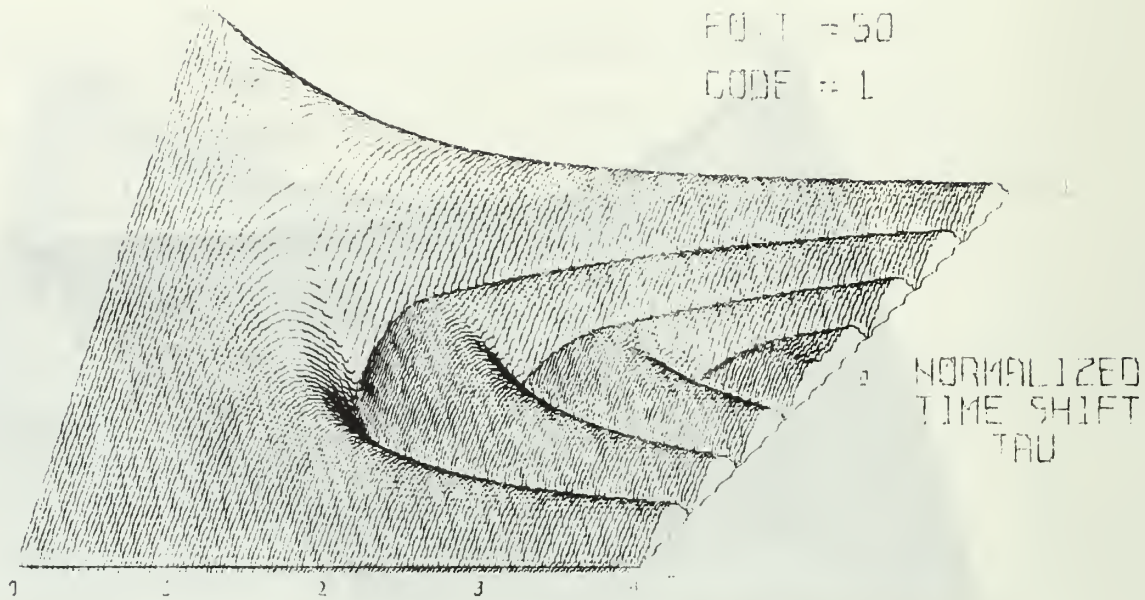

FIGURE 3-1C WIDEBAND AMBIGUITY FUNCTION

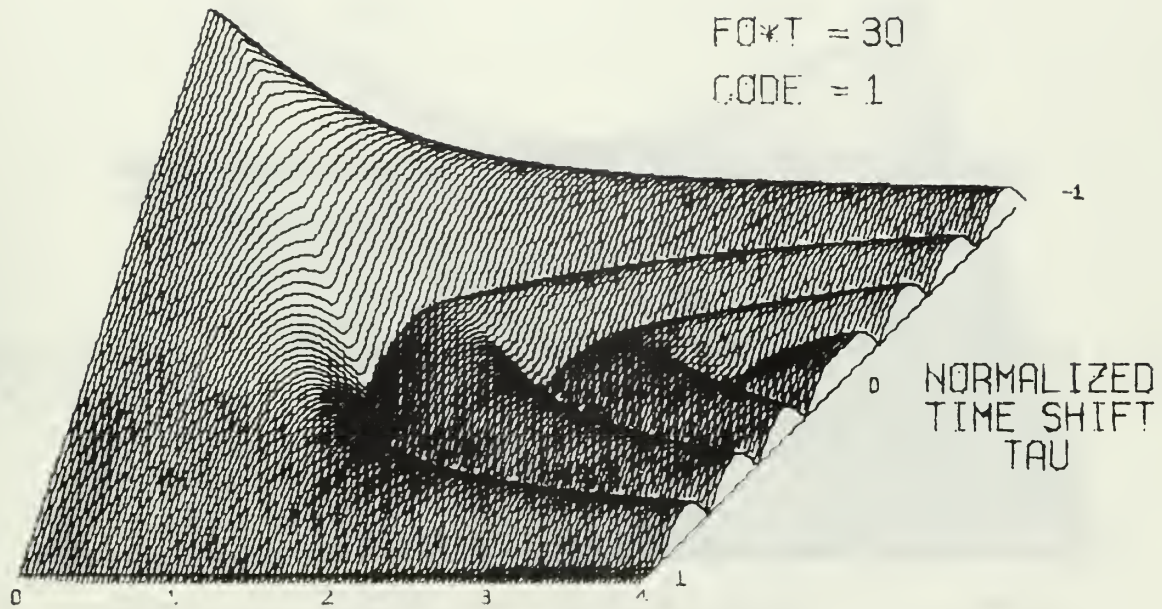

FIGURE 3-1D WIDEBAND AMBIGUITY FUNCTION

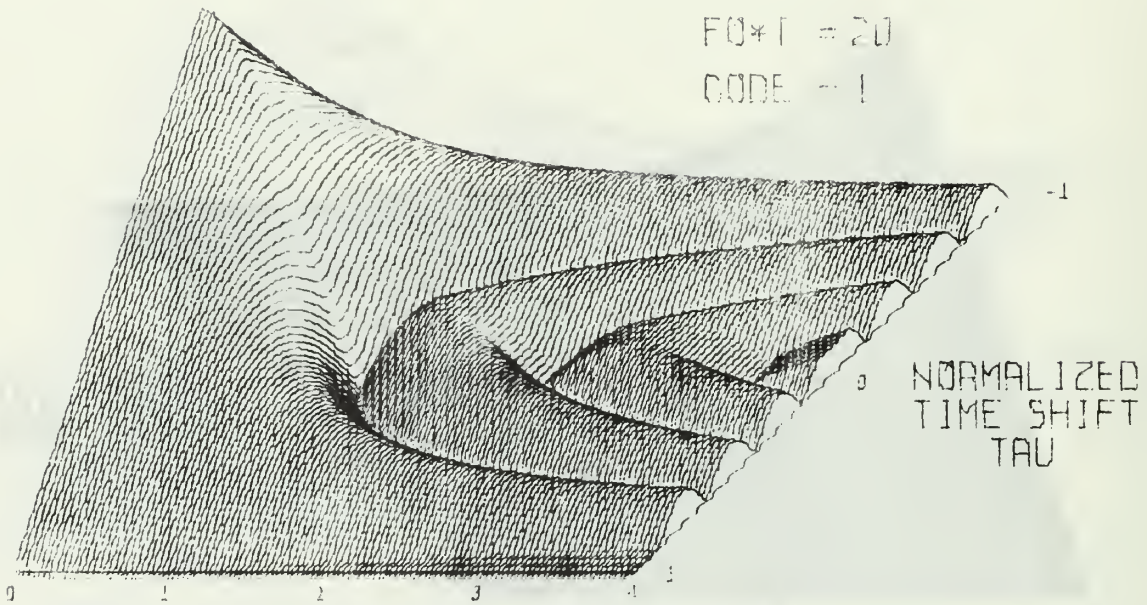

FIGURE 3-1E WIDEBAND AMBIGUITY FUNCTION

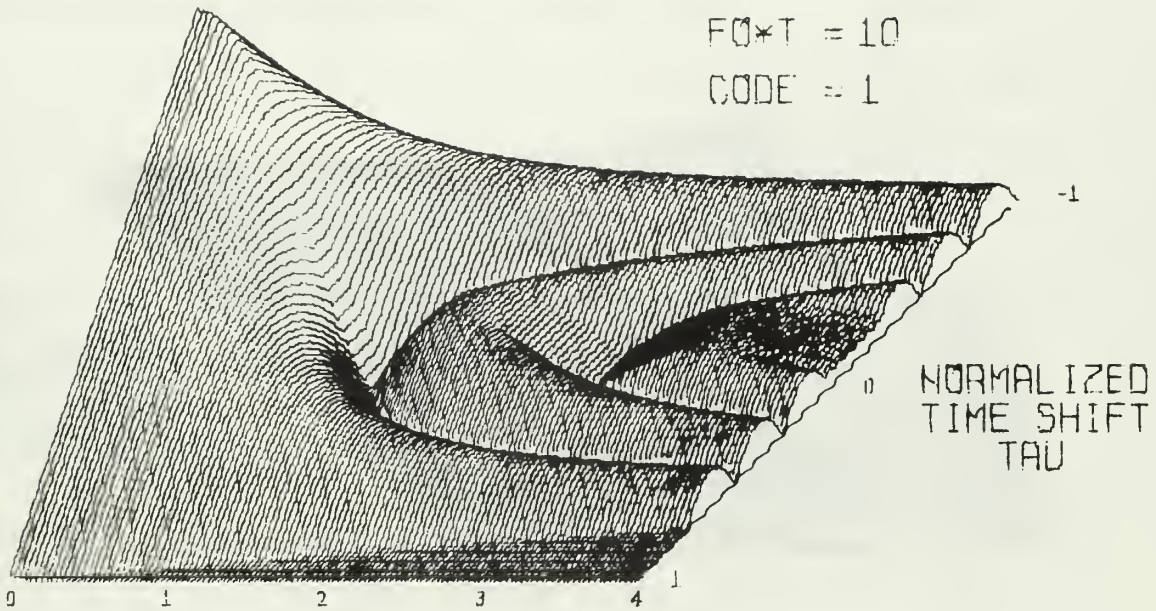

FIGURE 3-1F WIDEBAND AMBIGUITY FUNCTION

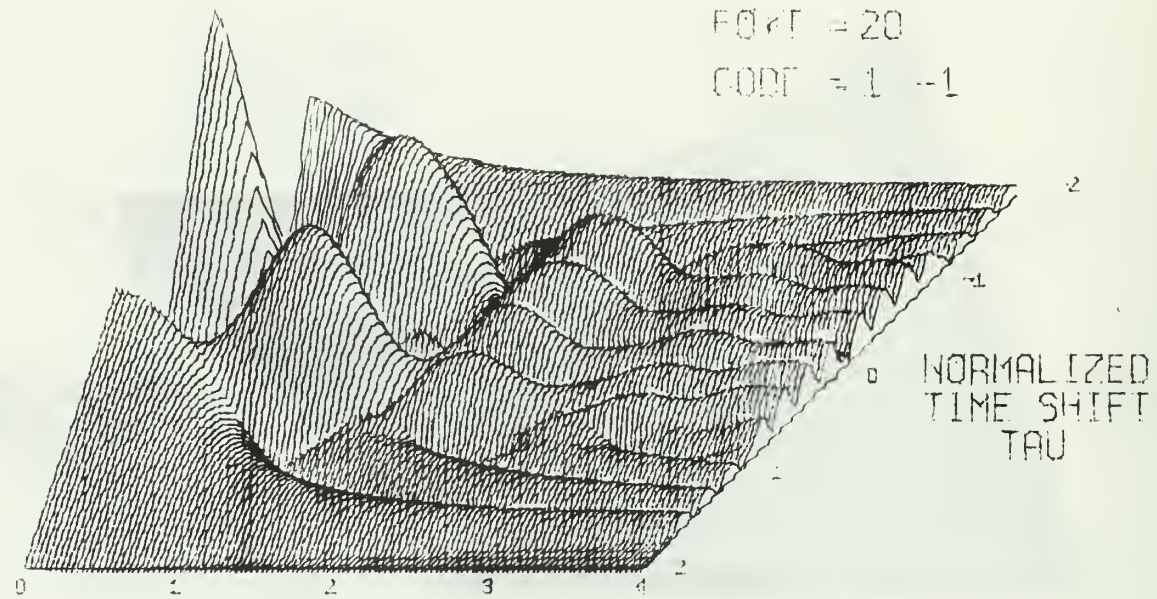

FIGURE 3-1 G WIDEBAND AMBIGUITY FUNCTION

IV. CONCLUSIONS

A. SUMMARY

The main objective of this thesis was to present the ambiguity function, in both the narrowband and wideband cases for selected Barker binary phase codes. Computer-generated three-dimensional projection drawings were presented for these Barker codes. In the narrowband case the computer-drawn ambiguity functions have shown much similarity to exist between the ambiguity functions of the Barker codes as the length of the code was increased. Also, as the code length increased the range and velocity resolution increased, while at the same time the ambiguities decreased. In the wideband case the effect of target motion was to shift the narrowband ambiguity function to a new axis of symmetry, and also to stretch the ambiguity function along the normalized doppler axis.

B. AREAS OF FUTURE STUDY

Barker codes are easy to generate and decode. As a result, the Barker codes have been used in some practical echo-ranging systems. Even though the study of wideband ambiguity functions is limited by the cases of practical interest in radar synthesis, it becomes very important in the case of sonar, where the velocity of propagation and signal carrier frequency are vastly reduced and large time-bandwidth products are required for accurate range and velocity determinations. In this respect, it may be beneficial to determine the wideband ambiguity functions for receding targets and also to study the symmetry of the wideband ambiguity functions.

BIBLIOGRAPHY

1. Woodward, P. M., Probability and Information Theory With Applications to Radar, McGraw-Hill, 1953.

2. Cook, C. E., Bernfeld, M. and Palmieri, C. A., "Matched Filtering, Pulse Compression and Waveform Design," Microwave Journal, pp. 73-81, January 1965.

3. Stanford Electronics Lab Report SEL-1602-1, Relativistic Theory of Wide-Bandwidth Radar, by J. L. Torres, March 1966.

4. Akita, R. M., An Investigation of the Narrow-band and Wideband Ambiguity Functions for Complimentary Codes, Master's Thesis, Naval Postgraduate School, Monterey, California, June 1968.

5. Siebert, W. M., "A Radar Detection Philosophy," IRE Transactions on Information Theory, Vol. IT-2, pp. 204-221, September 1956.

6. U. S. Naval Ordnance Laboratory, White Oak, Silver Spring, Maryland Report NOLTR 68-48, A CALCOMP Package for 3d Plotting, by D. J. Kennison, 1 April 1968.

7. Rihaczek, A. W., Principles of High-Resolution Radar, McGraw-Hill, 1969.

INITIAL DISTRIBUTION LIST

		No. Copies
1.	Defense Documentation Center Cameron Station Alexandria, Virginia 22314	20
2.	Library, Code 0212 Naval Postgraduate School Monterey, California 93940	2
3.	Naval Electronics Systems Command Department of the Navy Washington, D. C. 20390	1
4.	Professor C. F. Klamm, Jr. Department of Electrical Engineering Naval Postgraduate School Monterey, California 93940	7
5.	LTJG Jon P. Kjellander 2410 Washington St. Parsons, Kansas 67357	1

Security Classification

DOCUMENT CONTROL DATA - R & D

(Security classification of title, body of abstract and indexing annotation must be entered when the overall report is classified)

1. ORIGINATING ACTIVITY *(Corporate author)*
Naval Postgraduate School
Monterey, California 93940

2a. REPORT SECURITY CLASSIFICATION
UNCLASSIFIED

2b. GROUP

3. REPORT TITLE
Narrowband and Wideband Ambiguity Functions for Selected Barker Binary Phase Codes

4. DESCRIPTIVE NOTES *(Type of report and inclusive dates)*
Master's Thesis; October 1968

5. AUTHOR(S) *(First name, middle initial, last name)*
Jon Phillip Kjellander

6. REPORT DATE	7a. TOTAL NO. OF PAGES	7b. NO. OF REFS
October 1969	54	7

8a. CONTRACT OR GRANT NO.	9a. ORIGINATOR'S REPORT NUMBER(S)
b. PROJECT NO.	
c.	9b. OTHER REPORT NO(S) *(Any other numbers that may be assigned this report)*
d.	

10. DISTRIBUTION STATEMENT
This document has been approved for public release and sale; its distribution is unlimited.

11. SUPPLEMENTARY NOTES	12. SPONSORING MILITARY ACTIVITY
	Naval Postgraduate School Monterey, California 93940

13. ABSTRACT

The Barker binary phase codes have the interesting property that the magnitude of the range sidelobes never exceeds 1/N, where N is the code length. This thesis presents ambiguity functions for certain selected Barker binary phase codes in the form of computer-drawn three-dimensional projections. Both the narrowband and wideband cases are taken into consideration.

DD FORM 1 NOV 65 1473 (PAGE 1)

S/N 0101-807-6811

Security Classification

A-31408

14. KEY WORDS	LINK A		LINK B		LINK C	
	ROLE	WT	ROLE	WT	ROLE	WT
Barker Codes						
Signal Waveform Design						
Ambiguity Function						
Radar						
Sonar						